Upper Limit to Magnetism in LaAlO$_3$/SrTiO$_3$ Heterostructures

M. R. Fitzsimmons,[1] N. W. Hengartner,[1] S. Singh,[1,2] M. Zhernenkov,[1] F. Y. Bruno,[3] J. Santamaria,[3] A. Brinkman,[4]
M. Huijben,[4] H. J. A. Molegraaf,[4] J. de la Venta,[5] and Ivan K. Schuller[5]

[1]*Los Alamos National Laboratory, Los Alamos New Mexico 87545 USA*
[2]*Solid State Physics Division, Bhabha Atomic Research Center, Mumbai- 400085, India*
[3]*GFMC. Dpto. Fisica Aplicada III, Universidad Complutense de Madrid, 28040 Madrid. Spain*
[4]*MESA+ Institute for Nanotechnology, University of Twente, Enschede, The Netherlands*
[5]*Department of Physics and Center for Advanced Nanoscience, University of California San Diego, La Jolla, California 92093 USA*
(Received 2 August 2011; published 14 November 2011)

Using polarized neutron reflectometry we measured the neutron spin-dependent reflectivity from four
LaAlO$_3$/SrTiO$_3$ superlattices. Our results imply that the upper limit for the magnetization averaged over
the lateral dimensions of the sample induced by an 11 T magnetic field at 1.7 K is less than 2 G. SQUID
magnetometry of the neutron superlattice samples sporadically finds an enhanced moment, possibly due to
experimental artifacts. These observations set important restrictions on theories which imply a strongly
enhanced magnetism at the interface between LaAlO$_3$ and SrTiO$_3$.

In 2004, Ohtomo and Hwang [1] reported unusually high conductivity in LaAlO$_3$ and SrTiO$_3$ bilayer samples. Since then metallic conduction [1,2], superconductivity [3,4], magnetism, [5] and the coexistence of superconductivity and ferromagnetism [6] have been attributed to LaAlO$_3$/SrTiO$_3$ interfaces. On the other hand, the superconductivity of oxygen deficient bulk SrTiO$_3$ has been established for decades [7]. The conductivity in LaAlO$_3$/SrTiO$_3$ bilayers and superlattices [8] may arise from intrinsic effects such as the polar catastrophe [9,10], or extrinsic defects such as oxygen vacancies [11–14] or cation diffusion [15–17], and structural distortion or orbital reconstruction [18].

The presence of magnetic moments at the LaAlO$_3$/SrTiO$_3$ interface was inferred from the magnetoresistance of a (high O partial pressure grown) LaAlO$_3$/SrTiO$_3$ interface at low temperature in high magnetic fields [5,6,19]. The location and magnitude of magnetic moments in LaAlO$_3$/SrTiO$_3$ heterostructures remains unknown. Ferromagnetism (at room temperature), paramagnetism and diamagnetism (below 60 K) were claimed for 10 unit cells of LaAlO$_3$ on SrTiO$_3$ in fields up to 0.2 T [20]. Recent torque magnetometry measurements report moments $\sim 5 \times 10^{-10}$ Am^2 (equivalent to 5×10^{-7} G cm^3) for 5 unit cells of LaAlO$_3$ on SrTiO$_3$ [21]. If attributed to the entire LaAlO$_3$ film, then the saturation magnetization claimed from the measurements reported in the literature range between 10 and 126 G—a readily detectable signal with neutron scattering [22]. If attributed to just one unit at the LaAlO$_3$ on SrTiO$_3$ interface, then the magnetization is much larger. The large moments attributed to interfaces rely on measurement techniques that are unable to distinguish between interfacial and bulk magnetism [23,24]. Consequently, it is imperative to perform magnetic measurements which are

impervious to experimental artifacts suffered by bulk measurements [24], and to use techniques that are intrinsically sensitive to interface magnetism [25].

We have performed extensive polarized neutron reflectometry (PNR) measurements of LaAlO$_3$/SrTiO$_3$ superlattices. In spite of the fact that bulk measurements of the samples reported here imply a magnetization as high as 60 G, if attributed to the superlattice, PNR unequivocally establishes an upper limit of 2 G on their magnetization. The upper limit was obtained from measurements performed at fields as high as 11 T and temperatures as low as 1.7 K. The PNR results have serious implications for theories developed to explain magnetism in oxide superlattices [26–29].

LaAlO$_3$/SrTiO$_3$ superlattice samples were grown independently at laboratories located in Twente and Madrid. The Twente samples were grown on TiO$_2$ terminated (001) SrTiO$_3$ single-crystal substrates measuring 1 cm by 1 cm. [(LaAlO$_3$)$_8$/(SrTiO$_3$)$_{24}$]$_{30}$ (Twente1) and [(LaAlO$_3$)$_4$/(SrTiO$_3$)$_{12}$]$_{30}$ (Twente2) superlattices were fabricated by pulsed laser deposition with reflection high-energy electron diffraction (RHEED) control of the growth process. Single-crystal LaAlO$_3$ and SrTiO$_3$ targets were ablated at a laser fluence of 1.3 J/cm^2 and a repetition rate of 1 Hz with the substrate held at 850 °C in an oxygen environment at 2×10^{-3} mbar. RHEED intensity oscillations were observed during growth of each layer, consistent with layer-by-layer growth. After growth, the superlattices were cooled to room temperature in 2×10^{-3} mbar of oxygen at a rate of 10 °C/ min. Atomic force microscopy showed smooth terraces separated by unit cell high steps similar to the surface of the TiO$_2$-terminated (001) SrTiO$_3$ substrate. These conditions were identical to those previously used at Twente to grow heterostructures, (including superlattices) with conducting LaAlO$_3$/SrTiO$_3$ interfaces [8,30].

$[(LaAlO_3)_8/(SrTiO_3)_{24}]_{30}$ (Madrid2) and $[(LaAlO_3)_4/(SrTiO_3)_{12}]_{15}$ (Madrid1) were grown on TiO_2 terminated (001) $SrTiO_3$ substrates using high-pressure (2.9 mbar) pure oxygen sputtering at a substrate temperature of 750 °C. After growth the samples were cooled to 600 °C. At this temperature the chamber was filled with 900 mbar O_2, and the samples were annealed for 5 minutes at 550 °C before cooling to room temperature at a 20 °C/ min rate.

The physical structure of the superlattice is determined from the wave vector transfer (Q)-dependence of the X-ray reflectivity which is sensitive to the uniformity of layer thicknesses and interface roughness. The broadening of the superlattice Bragg reflections implies that the layer thicknesses varied the sample (along its surface normal) by more than half a unit cell. Furthermore, the superlattice Bragg reflections for Madrid1 and Twente2 were shifted slightly towards larger Q compared to the simulation, implying the $LaAlO_3$ layer thicknesses for these samples may be (3.5 ± 0.5) unit cells thick rather than the intended 4. On the other hand, the $LaAlO_3$ thickness of Samples Twente1 and Madrid2 were closer to the intended 8 unit cells.

To test whether the sporadic bulk magnetic signals of up to 60 G from the samples reported here originate from the $LaAlO_3/SrTiO_3$ heterostructures [31], we measured the depth dependence of magnetization for several $LaAlO_3/SrTiO_3$ superlattices at different fields and temperatures with PNR [32–34]. In PNR the intensity of the specularly reflected neutron beam is compared to the intensity of the incident beam as a function of Q and neutron beam polarization. The specular reflectivity, R, is

determined by the neutron scattering length density depth profile, $\rho(z)$, averaged over the lateral dimensions of the sample. $\rho(z)$ consists of nuclear and magnetic scattering length densities such that $\rho_{\pm}(z) = \rho_n(z) \pm CM(z)$, where $C = 2.853 \times 10^{-9} \text{ Å}^{-2}\text{G}^{-1}$ and $M(z)$ is the depth profile of the magnetization (in G) parallel to the applied field [34]. The $+(-)$ sign denotes neutron beam polarization along (opposite to) the applied field. Thus, by measuring $R^+(Q)$ and $R^-(Q)$, $\rho_n(z)$ and $M(z)$ can be obtained separately.

The origin of the spin dependence of $\rho_{\pm}(z)$ is the magnetic induction B [35]. Neutron scattering requires a degree of coherence of the neutron beam but does not require coherence of magnetic spins (long range or not). For examples of applications of neutron scattering to measure B in materials lacking long range order of magnetic spins or even lacking magnetic spins all together see Ref. [36] (paramagnetic moments in V) and Ref. [37] (skin depth of conventional superconductors). In the case of laterally nonuniform magnetism as observed recently by J. A. Bert *et al.* [38] in a $LaAlO_3/SrTiO_3$ bilayer, the spin dependence of $R^{\pm}$ would be affected by the magnetization of the magnetic entities weighted by the ratio of the total lateral area of the entities to the lateral dimensions of the sample. Figure 1 of Ref. [38] shows this ratio to be $\sim 9\%$.

The difference between $R^+(Q)$ and $R^-(Q)$ or the difference divided by the sum, a ''spin asymmetry'', is very sensitive to small M values. A major advantage of PNR is the ability to distinguish magnetism at an interface or a thin film from the substrate. Measurements of the spin-dependent superlattice Bragg reflection assure that variations of M having the period of the superlattice are detected and not spurious contamination from extrinsic sources.
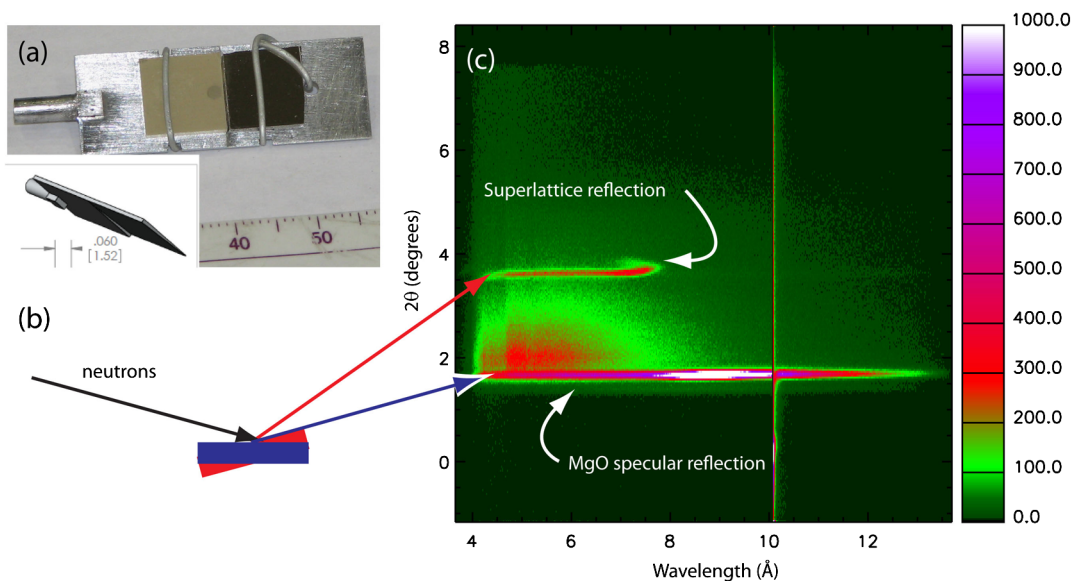

FIG. 1 (color online). (a) Device used to simultaneously hold the control and $LaAlO_3/SrTiO_3$ samples during the PNR experiment. (b) Schematic showing reflection of the neutron beam by the control (blue) and neutron sample (red). (c) Neutron intensity image for one beam polarization at 11 T and 1.7 K from Twente1.

Thus, concerns regarding bulk magnetometry of nano-scaled materials [24] are not germane to PNR.

Detection of small M can be problematic for PNR. First, the difference between R^+ and R^- may be so small that it is not statistically significant. The difference can be sub-stantially enhanced using a superlattice, where many inter-faces contribute to the intensity of the superlattice Bragg reflection.

Superlattices also offer advantages for detection of inter-face magnetism with magnetometry. For example, the possible interfacial magnetism in $LaAlO_3/SrTiO_3$ hetero-structures maybe enhanced in a superlattice, even if the signal does not scale with the number of interfaces. For instance different interfaces may contribute differently to the magnetic signal because the interfacial roughness of $LaAlO_3$ grown on $SrTiO_3$ may be different than that of $SrTiO_3$ grown on $LaAlO_3$ [9].

A second challenge faced by neutron scattering is the bias the neutron spectrometer may induce in one spin state over the other. For example, to reverse the neutron beam polarization a neutron spin flipper is turned off or on, thus, treating the two polarizations differently perhaps inducing a systematic error on R^+ or R^-. Previously, we have shown the instrumental bias for the Asterix reflectometer or dif-fractometer to be less than one part in 1000 [39].

To further suppress instrumental bias, we developed an innovative measurement protocol. Two samples measured simultaneously were compared—a $LaAlO_3/SrTiO_3$ super-lattice, and a control (a MgO single crystal). The samples were mounted on a special holder with approximately $1°$ difference between their surface normals [Figs. 1(a) and 1(b)]. Thus, the specularly reflected beams corre-sponding to the superlattice Bragg reflection from the $LaAlO_3/SrTiO_3$ and the region of total reflection from the control sample appear in different locations of a posi-tion sensitive neutron detector [Fig. 1(c)]. The neutron intensity was measured as a function of wavelength λ for fixed scattering angle 2θ from which $Q = 4\pi \frac{\sin\theta}{\lambda}$. The incident beam intensity for each spin state was determined using a portion of the spectrum of the neutron beam reflected by the control. This protocol normalizes out in-strumental artifacts that might produce a false spin asym-metry, since the sample and control are measured simultaneously.

Samples and control were cooled in an 11 T field from room temperature to 1.7 K. The spin-dependent reflectiv-ities were simultaneously recorded as functions of field and temperature using the Asterix spectrometer at LANSCE. The data were corrected for variation of the neutron spec-trum and wavelength dependent efficiencies of the neutron polarizer and spin flipper [40].

The main panel of Fig. 2(a) shows the reflectivity of sample Twente1 near the region of total reflectivity. Reflectivity data are sensitive to variation of $\rho \pm (z)$ with length scales of $\sim 2\pi/Q_{max}$ (where Q_{max} is the maximum
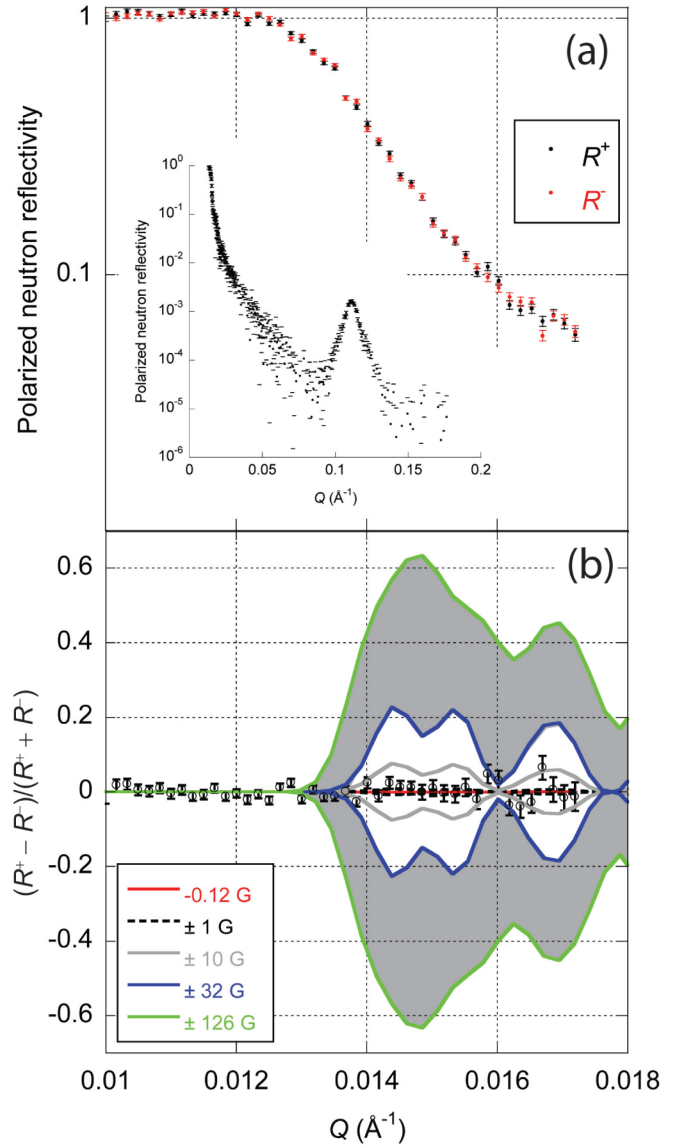

FIG. 2 (color online). (a) Polarized neutron reflectivity from Twente1 near the critical edge and (inset) R^+ from Madrid1 over a broader range of Q showing the superlattice Bragg reflection at $Q = 0.12$ Å^{-1}. (b) Spin asymmetry of the neutron reflectivity of Twente1 near the critical edge (1-sigma errors). Curves show the spin asymmetry for various uniformly distributed magnetization in the superlattice. Magnetization reports from $LaAlO_3/SrTiO_3$ bilayers, if attributed to the $LaAlO_3$ layer, all exceed the 10 G curve.

Q measured). Since the data shown in the main panel Fig. 2(a) correspond to small Q, they are sensitive to the net magnetization of the superlattice. On the other hand, the large-Q superlattice Bragg reflections such as in the inset are sensitive to variation of $M(z)$ across the superlat-tice. Consequently, the data in the main panel of Fig. 2(a) were fitted to a model that assumed a uniform magnetiza-tion depth profile in the superlattice in order to establish an upper limit of its net magnetization. The (-0.12 ± 1.2) G

obtained implies a statistically insignificant spin asymmetry determined from the critical edge of the LaAlO$_3$/SrTiO$_3$ (near $Q_c = 0.0133$ Å^{-1}). The influence on the spin asymmetry [41] of magnetization equal to -0.12, ± 1, ± 10, ± 32 and ± 126 G is shown by the red, dashed, light gray, blue, and green curves in Fig. 2(b), respectively. The 32 and 126 G curves (bounding the gray-shaded region) were chosen based on the data and volume of the LaAlO$_3$ film reported in Refs. [20,42] The light gray curves correspond to 5×10^{-10} Am^2 (equivalent to 5×10^{-7} G cm^3) reported in Ref. [21], if the moment is attributed to the LaAlO$_3$ layer. We show positive and negative values of M, in case M is diamagnetic. Our neutron scattering data are unequivocally inconsistent with previous reports of magnetization of LaAlO$_3$/SrTiO$_3$ heterostructures, if the magnetization inferred from bilayers is present in the superlattice, or with the magnetization (as large as 60 G) of our samples, if attributed to the superlattice, as obtained with magnetometry [31].

To quantify the $M(z)$ variations across the LaAlO$_3$/SrTiO$_3$ superlattice as functions of field and temperature, we measured the intensities of the neutron spin dependence of the first order superlattice Bragg reflection. An example for one neutron beam polarization and one sample (Madrid1) is shown in the inset of Fig. 2(a). We defined the Spin Asymmetry Ratio (SAR) equal to the difference between the *integrated intensities* of the spin-dependent superlattice Bragg reflections divided by their sum [43]. Figure 3 shows the SAR for Twente1 as a

function of field for two temperatures averaged from two separate experiments. Figure 4 shows the SAR for four samples measured at 11 T and 1.7 K. The spin asymmetry of the superlattice Bragg reflection is sensitive to changes of magnetization having the period of the superlattice. It is possible for such changes to be too small to produce spin asymmetry at the critical edge. For example, because the magnetization may change sign as a function of depth, or it may be confined to a fraction of the superlattice.

The lines in Fig. 3 were obtained from weighted least squares fits to the data. The slope of the 1.7 K data (closed symbols, Fig. 3), $(-0.0006 \pm 0.0002)\, T^{-1}$ (1-sigma error) is statistically different than zero and suggests that the SAR becomes more negative as the field increases. The slope for the 80 K data (open symbols, Fig. 3), $(-0.0003 \pm 0.0003)\, T^{-1}$ is zero within statistical error.

To set an upper limit on the magnetization change across the interface LaAlO$_3$/SrTiO$_3$ in the superlattices, we related the SAR to the magnetization in absolute units. The SAR for our samples depends linearly on the change of magnetization across the LaAlO$_3$/SrTiO$_3$ interface and is used to calibrate the right-hand axes of Figs. 3 and 4. If the magnetization is along the applied field, a negative SAR implies that the magnetization in SrTiO$_3$ is greater than that of LaAlO$_3$. For Sample Twente1 at 11 T and 1.7 K, the SAR is about -0.005 which implies that the SrTiO$_3$ magnetization is ~ 2 G, if the magnetization of LaAlO$_3$ is assumed to be zero. As a consequence, the thickness-weighted average magnetizations of the SrTiO$_3$ and
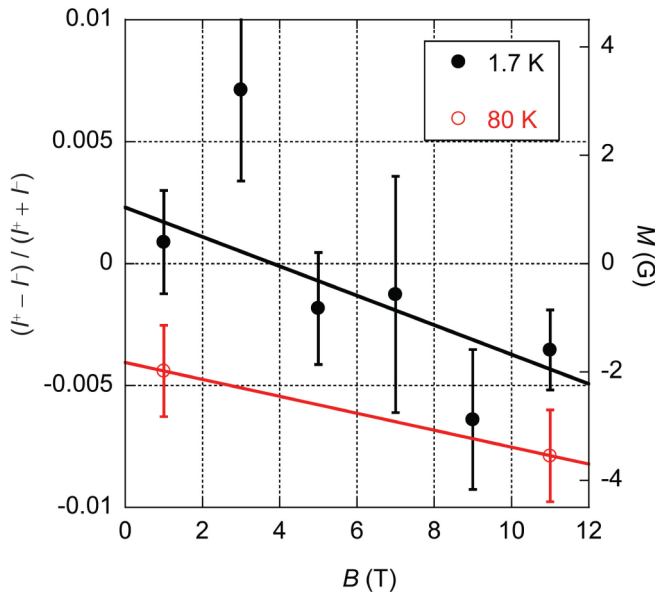

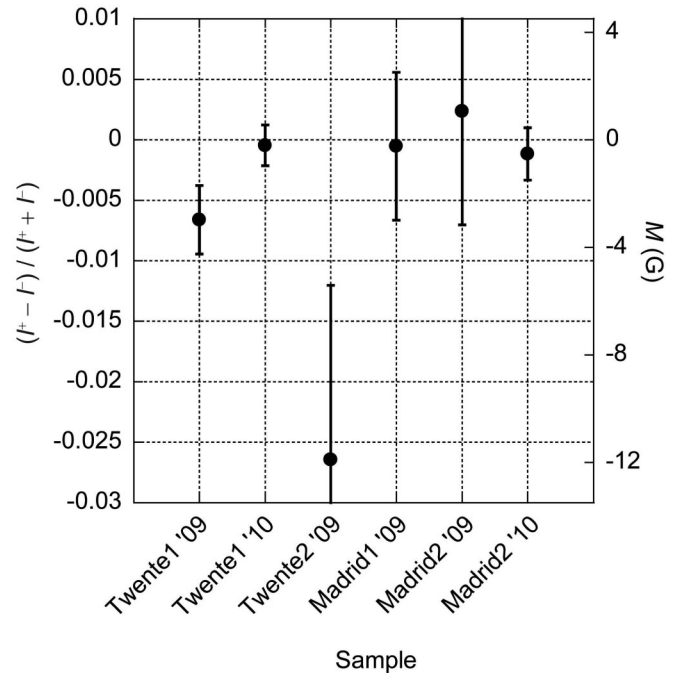FIG. 3 (color online). Ratio of the difference over the sum of the integrated intensities, SAR, of the spin-dependent superlattice Bragg reflections (1-sigma errors) for Twente1 as functions of field and temperature. The method for obtaining M from $(I^+ - I^-)/(I^+ + I^-)$ is discussed in the text.

FIG. 4. Ratio of the difference over the sum of the integrated intensities, SAR, of the spin-dependent superlattice Bragg reflections (1-sigma errors) for different samples at 11 T and 1.7 K.

LaAlO$_3$ layers are below the upper limit set (~ 1 G) by the absence of spin asymmetry at the critical edge.

Alternatively, if the magnetization is opposite to the applied field, i.e., diamagnetic, a negative SAR implies that the magnetization resides in the LaAlO$_3$ layer. Our measurements cannot distinguish between paramagnetism in SrTiO$_3$, or diamagnetism in LaAlO$_3$.

Scattering from the first order superlattice Bragg reflection corresponds to length scales equal to the period of the superlattice—a few unit cells. Measurements of higher order superlattice Bragg reflections would be required to identify localization of the magnetization to a single unit cell at the LaAlO$_3$/SrTiO$_3$ interface.

Overall the SAR of the superlattice Bragg reflection together with measurements near the critical edge imply that: the magnetization in the LaAlO$_3$ layer (averaged over its lateral dimensions) is ~ 2 G less than that of the SrTiO$_3$ layer, the magnetization of one of these layers is near zero, and the variation of magnetization with depth has the period of the superlattice. If attributed to Ti, the 2 G upper limit for the magnetic moment would correspond to 0.7% of Ti^{3+} per unit cell perhaps arising from the few percent Ti $3d_{xy}$ electrons reported by x-ray spectroscopy. [18,44]

In conclusion, we established an upper limit of 2 G for the magnetization change across the LaAlO$_3$/SrTiO$_3$ interfaces (laterally averaged) in superlattices at 11 T and 1.7 K. The upper limit was obtained from differences between the integrated intensities of the superlattice Bragg reflections for neutron beam polarization along and opposite to the applied field. No significant spin difference was measured near the critical edge of the LaAlO$_3$/SrTiO$_3$ superlattice. Thus, the magnetization *averaged over the entire superlattice* is likely to be less than the upper limit of ~ 1 G inferred from measurement of the MgO control, and certainly less for fields smaller than 11 T. These results place strong constraints on theories of magnetism in LaAlO$_3$/SrTiO$_3$ heterostructures.

[1] A. Ohtomo and H. Y. Hwang, Nature (London) **427**, 423 (2004).
[2] S. Thiel *et al.*, Science **313**, 1942 (2006).
[3] N. Reyren *et al.*, Science **317**, 1196 (2007).
[4] S. Gariglio *et al.*, J. Phys. Condens. Matter **21**, 164213 (2009).
[5] A. Brinkman *et al.*, Nature Mater. **6**, 493 (2007).
[6] D. A. Dikin *et al.*, Phys. Rev. Lett. **107**, 056802 (2011).
[7] J. F. Schooley, W. R. Hosler, and M. L. Cohen, Phys. Rev. Lett. **12**, 474 (1964).
[8] M. Huijben *et al.*, Nature Mater. **5**, 556 (2006).
[9] N. Nakagawa *et al.*, Nature Mater. **5**, 204 (2006).
[10] For a review see, J. N. Eckstein, Nature (London) **6**, 473 (2007).
[11] K. Yoshimatsu *et al.*, Phys. Rev. Lett. **101**, 026802 (2008).
[12] S. A. Chambers, Phys. Rev. Lett. **102**, 199703 (2009).
[13] K. Yoshimatsu *et al.*, Phys. Rev. Lett. **102**, 199704 (2009).
[14] A. Kalabukhov *et al.*, Phys. Rev. B **75**, 121404(R) (2007).
[15] P. R. Willmott *et al.*, Phys. Rev. Lett. **99**, 155502 (2007).
[16] A. S. Kalabukhov *et al.*, Phys. Rev. Lett. **103**, 146101 (2009).
[17] A. Kalabukhov *et al.*, Europhys. Lett. **93**, 37001 (2011).
[18] M. Salluzzo *et al.*, Phys. Rev. Lett. **102**, 166804 (2009).
[19] M. Ben Shalom *et al.*, Phys. Rev. B **80**, 140403 (2009).
[20] Ariando *et al.*, Nature Commun. **2**, 188 (2011).
[21] L. Li, C. Richter, J. Mannhart, and R. C. Ashoori, Nature Phys. **7**, 762 (2011).
[22] B. J. Kirby *et al.*, IEEE Trans. Magn. **43**, 3016 (2007).
[23] J. M. D. Coey and S. A. Chambers, Mater. Res. Bull. **33**, 1053 (2008).
[24] M. A. Garcia *et al.*, J. Appl. Phys. **105**, 013925 (2009).
[25] M. R. Fitzsimmons *et al.*, J. Magn. Magn. Mater. **271**, 103 (2004).
[26] K. Janicka, J. P. Velev, and E. Y. Tsymbal, J. Appl. Phys. **103**, 07B508 (2008).
[27] N. Pavlenko *et al.*, arXiv:1105.1163.
[28] K. Micheali, A. C. Potter, and P. A. Lee, arXiv:1107.4352.
[29] S. Okamoto, A. J. Millis and N. A. Spaldin, Phys. Rev. Lett. **97**, 056802 (2006).
[30] R. Pentcheva *et al.*, Phys. Rev. Lett. **104**, 166804 (2010).
[31] See Supplemental Material at http://link.aps.org/supplemental/10.1103/PhysRevLett.107.217201 for magnetization data for our samples.
[32] G. P. Felcher *et al.*, Rev. Sci. Instrum. **58**, 609 (1987).
[33] C. F. Majkrzak, Physica (Amsterdam) **221B**, 342 (1996).
[34] M. R. Fitzsimmons and C. Majkrzak, *Modern Techniques for Characterizing Magnetic Materials* (Springer, New York, 2005), Chap. 3, p. 107.
[35] F. Mezei, Physica (Amsterdam) **356B**, 64 (2005).
[36] C. G. Shull and R. P. Ferrier, Phys. Rev. Lett. **10**, 295 (1963).
[37] G. P. Felcher, Physica (Amsterdam) **192B**, 137 (1993).
[38] J. A. Bert *et al.*, Nature Phys. **7**, 767 (2011).
[39] M. R. Fitzsimmons *et al.*, Phys. Rev. B **76**, 245301 (2007).
[40] In the limit polarization P goes to 1, the true spin difference is related to the observed spin difference by the factor $\frac{2}{1+P}$. $P > 0.93$ for our experiment.
[41] L. G. Parratt, Phys. Rev. **95**, 359 (1954).
[42] For example, the low temperature field cooled moment for a 10 unit cell thick LaAlO$_3$ film on a 5 mm by 5 mm SrTiO$_3$ is shown in Fig. 1 of Ref. [20] to be $\sim 12 \times 10^{-6}$ G cm^3.
[43] The integration was performed over a region corresponding to 2 times the root mean square (rms) width of the peak from its center.
[44] M. Sing *et al.*, Phys. Rev. Lett. **102**, 176805 (2009).